Modified EWMA Chart with Restarting Mechanism for Monitoring Serially Correlated Sequential Processes

Zibo Tian and Peihua Qiu*

Department of Biostatistics, University of Florida

2004 Mowry Road, Gainesville, FL 32610, U.S.A.

Email: pqiu@ufl.edu; *Telephone*: (+1) 352-294-5911; *Fax*: (+1) 352-294-5931

Abstract

In practical applications of statistical process control (SPC), the assumption of data independence among serial process observations is often unrealistic. In the SPC literature, it has been well demonstrated that control charts ignoring the serial data correlation would be unreliable to use. Thus, it is important to develop control charts that can accommodate serial data correlation properly. To this end, one approach is to decorrelate the observed data properly before a control chart is used. However, the related computing burden would be too heavy to be practically feasible if the observed data at the current observation time need to be decorrelated with all previous data. With a cumulative sum (CUSUM) chart, its restarting mechanism has been found helpful to reduce the computing burden substantially by ignoring the observed data collected before the previous restarting time. In many applications, e.g., those with unequally spaced observation times, exponentially weighted moving average (EWMA) charts are often preferred since construction of their charting statistics can accommodate the unequally spaced observation times well. But, conventional EWMA charts do not have the restarting mechanism, and thus are difficult to use in cases with serially correlated data. To address this issue, a modified EWMA chart is considered in this paper to include the restarting mechanism in the chart. Numerical studies confirm that the computing time using the modified EWMA chart is dramatically reduced for monitoring serially correlated data while its process monitoring performance is little compromised.

Key Words: Computing time; Decorrelation; EWMA chart; Masking effect; Restarting mechanism; Serial data correlation.

1 Introduction

Statistical process control (SPC) charts have been used broadly in practice for online monitoring of sequential processes (Hawkins and Olwell, 1998; Montgomery, 2019; Qiu, 2014). Traditional SPC charts, such as the cumulative sum (CUSUM) and exponentially weighted moving average (EWMA) charts, assume that the in-control (IC) process observations at different time points are independent. While this assumption might be (approximately) valid in the manufacturing industry, they are rarely valid in environmental monitoring, disease surveillance, and many other applications where serial correlation among the observed data is often non-negligible. This paper focuses on online monitoring of processes with serially correlated data.

In the existing literature, there have been some discussions on process monitoring of serially correlated data. In the case of monitoring univariate continuous processes, a number of methods have been developed based on parametric time series models and sequential monitoring of the resulting residuals, or on adjustment of the control limits of the conventional control charts (cf., Apley and Tsung, 2002; Capizzi and Masarotto, 2008; Kim et al., 2007; Lee and Apley, 2011; Runger and Willemain, 1995; Zhang, 1998). Qiu et al. (2020) proposed a method for monitoring processes with stationary and short-ranged serial correlation without using parametric time series models. That method decorrelated the observed data first, and then applied a CUSUM chart to the decorrelated data. To reduce computing burden and data storage requirement, the restarting mechanism of the CUSUM chart was used by ignoring all observations collected before the previous restarting time when decorrelating the observed data at the current time point with all previous data. As demonstrated in You and Qiu (2019), another benefit to decorrelate the observed data at the current time point with less previous data is that the following shift masking effect could be substantially reduced. Since decorrelated data are typically linear combinations of the original process observations, a process mean shift in the original observations would be attenuated in the

decorrelated data and the degree of attenuation could be reduced greatly if the current process observations need to be decorrelated with a small amount of previous data only.

In practice, people often prefer to use the EWMA chart because it is relatively easy to devise, i.e., setting up the mean, variance, asymptotic distribution, and control limit for the EWMA charting statistic, as compared to the CUSUM chart. In addition, in applications when the observation times are unequally spaced, it has been found that the EWMA chart is relatively easy to be adapted properly in its construction to accommodate the unequally spaced observation times (e.g., Qiu et al., 2018; You and Qiu, 2020). However, when the conventional EWMA chart is used for monitoring processes with correlated data, it could have the following difficulty. On one hand, the serial correlation should be accommodated properly, and the results could be unreliable otherwise (cf., Apley and Tsung, 2002; Runger and Willemain, 1995). On the other hand, the computing and data storage demands would be prohibitive if the observed data at the current time need to be decorrelated with all previous data, since the conventional EWMA chart does not have the restarting mechanism. In the SPC literature, several modified versions of the EWMA chart have been suggested for solving various SPC problems. For instance, Crowder and Hamilton (1992) developed a one-sided EWMA chart for monitoring process standard deviation by resetting the EWMA statistic to zero whenever it becomes negative, which is intuitively reasonable because the process standard deviation cannot be negative. A similar modified EWMA chart was discussed in Gan (1998) for monitoring the incidence rate of some rare events. However, it has not been studied carefully how the EWMA chart can be modified properly for monitoring processes with correlated data so that the computing time and data storage demand are both manageable while the performance of the modified EWMA chart is not substantially sacrificed. Because the observed data of most processes in practice are serially correlated, this problem is important, although it has not been addressed carefully yet.

In this paper, we study the performance of a modified EWMA chart equipped with the restarting mechanism for monitoring processes with serially correlated observations. Before the modified

chart is used, the observed data at the current time point need to be decorrelated with all previous data collected after the previous restarting time. Because the time length from the previous restarting time to the current time, which is called *sprint length* in Chatterjee and Qiu (2009) for a CUSUM chart, is usually a single-digit integer, the computing time and data storage demand would be both small for such data decorrelation. Numerical studies show that the performance of the modified EWMA chart would not be sacrificed much for the inclusion of the restarting mechanism compared to the conventional EWMA chart used after the current data are decorrelated with all previous data, while the computing time of the former is negligible compared to that of the latter.

The remainder of the paper is organized as follows. Section 2 describes the modified EWMA chart in detail. Some simulation results to evaluate its performance in comparison with some alternative control charts are presented in Section 3. A real-data example for demonstrating the modified EWMA chart is discussed Section 4. Several concluding remarks are given in Section 5. A few extra numerical results are provided in Appendix.

2 Methodology

2.1 Modified EWMA Chart with Restarting Mechanism for Monitoring Correlated Data

Assume that $\{X_1, X_2, \ldots, X_i\}$ are process observations collected up to the current observation time i for process monitoring. Then, the traditional EWMA charting statistic for the task of monitoring process mean shifts is defined to be

$$E_{X,i} = \lambda \frac{X_i - \mu}{\sigma} + (1-\lambda) E_{X,i-1}, \qquad \text{for } i \geq 1, \tag{1}$$

where $E_{X,0} = 0$, $\lambda \in (0, 1]$ is a weighting parameter, μ is the IC process mean, and σ is the IC process standard deviation. In cases when the IC process distribution is normal and process

observations are independent at different observation times, it is easy to check that the asymptotic distribution of $E_{X,i}$ is $N(0, \lambda/(2-\lambda))$. Therefore, to detect an upward process mean shift, the EWMA chart gives a signal when

$$E_{X,i} > \rho_1, \tag{2}$$

where $\rho_1 > 0$ is a control limit chosen to achieve a pre-specified IC ARL (ARL_0) value. The chart for detecting a downward or arbitrary mean shift can be defined in a similar way.

Motivated by scenarios for monitoring quantities with special ranges (e.g., process standard deviation in the range $[0, \infty)$), a modified version of the one-sided EWMA chart (1)-(2) with a restarting mechanism has been proposed in the literature (cf., Crowder and Hamilton, 1992; Gan, 1998). Its charting statistic is defined to be

$$E^+_{X,i} = \max\left\{0, \lambda\frac{X_i - \mu}{\sigma} + (1-\lambda)E^+_{X,i-1} - k\right\}, \qquad \text{for } i \geq 1, \tag{3}$$

where $E^+_{X,0} = 0$, λ is similar to the one in Expression (1), and $k \geq 0$ is similar to the allowance parameter in the conventional CUSUM chart. A signal of an upward mean shift is given when

$$E^+_{X,i} > \rho_2, \tag{4}$$

where $\rho_2 > 0$ is a control limit. In (3), the charting statistic $E^+_{X,i}$ is reset to 0 each time when $\lambda(X_i - \mu)/\sigma + (1-\lambda)E^+_{X,i-1} \leq k$, indicating that the updated EWMA statistic at time i is small since k is usually chosen small. This is the restarting mechanism discussed in the literature (cf., Qiu 2014, Chapter 4).

While the control charts (1)-(2) and (3)-(4) are designed for monitoring processes with independent data, it has been well demonstrated in the literature that their performance would be unreliable in cases when processes observations are serially correlated (e.g., Qiu 2014, Chapter 5). To address this issue, one solution is to decorrelate the observation at the current time point with all previous data and then monitor the decorrelated data with the control charts. However, the heavy burden of

computing time and data storage demand would make this approach infeasible as the observation time i increases. To overcome this difficulty, we suggest incorporating the concept of sprint length into data decorrelation for online process monitoring. This idea was first discussed in Chatterjee and Qiu (2009) and has been applied to different versions of the CUSUM chart (cf., Li and Qiu, 2020; Qiu et al., 2020; You and Qiu, 2019; Qiu and Xie, 2022). At the current observation time i, the sprint length $S_{X,i}$ of the chart (3)-(4) is defined to be

$$S_{X,i} = \begin{cases} 0, & \text{if } E^+_{X,i} = 0, \\ s, & \text{if } E^+_{X,i-s} = 0, E^+_{X,i-s+1} \neq 0, \ldots, E^+_{X,i} \neq 0, \end{cases}$$

where $1 \leq s \leq i$ is an integer. Clearly, $S_{X,i}$ is the number of observation times from the previous restarting time to the current time i, and the charting statistic $E^+_{X,i}$ at the current time i depends on the previous $S_{X,i-1}$ observations only. Because the process observations collected before the previous restarting time do not contain much evidence for an upward mean shift and have been ignored in subsequent process monitoring, the current observation X_i only needs to be decorrelated with its previous $S_{X,i-1}$ observations collected after the previous restarting time.

In the proposed modified EWMA chart, its sprint length is defined based on its charting statistic values which in turn are calculated from the decorrelated data. The related quantities are defined below.

- When $i = 1$, set $S_{X^*,0} = 0$ and define the standardized observation to be

$$X^*_1 = (X_1 - \mu)/\sqrt{\sigma_{11}},$$

  where $S_{X^*,j}$ denotes the sprint length at j, for $j \geq 0$, and $\sigma_{11} = \text{var}(X_1)$ is the IC variance. Then, the charting statistic is defined to be

$$E^+_{X^*,1} = \max\left\{0, \lambda X^*_1 - k\right\}, \tag{5}$$

where $\lambda \in (0, 1]$ is the weighting parameter and $k \geq 0$ is the allowance constant. If $E^+_{X^*,1} = 0$, then define $S_{X^*,1} = 0$. Otherwise, define $S_{X^*,1} = 1$.

- When $i \geq 2$, the following two cases are considered. If $S_{X^*,i-1} = 0$, then X^*_i is defined to be the standardized version of X_i. Namely,

$$X^*_i = (X_i - \mu)/\sqrt{\sigma_{ii}},$$

where $\sigma_{ii} = \text{var}(X_i)$ is the IC variance. If $S_{X^*,i-1} > 0$, then we need to decorrelate X_i with $S_{X^*,i-1}$ previous observations. To this end, let $\mathbf{Z}_i = (X_{i-S_{X^*,i-1}} - \mu, \ldots, X_{i-1} - \mu, X_i - \mu)^T$. The covariance matrix of $\mathbf{Z}_i$ can be written as

$$\mathbf{\Sigma}_{i,i} = \begin{pmatrix} \mathbf{\Sigma}_{i-1,i-1} & \mathbf{V}_{i-1,i} \\ \mathbf{V}^T_{i-1,i} & \sigma_{ii} \end{pmatrix},$$

where $\mathbf{V}_{i-1,i} = (\sigma_{i-S_{X^*,i-1},i}, \ldots, \sigma_{i-1,i})^T$, and $\sigma_{ji} = \text{cov}(X_j, X_i)$, for $j = i-S_{X^*,i-1}, \ldots, i-1$. By the Cholesky decomposition of $\mathbf{\Sigma}_{i,i}$, we have

$$\mathbf{\Phi}_i \mathbf{\Sigma}_{i,i} \mathbf{\Phi}^T_i = \mathbf{D}_i,$$

where $\mathbf{\Phi}_i$ is a lower-triangular matrix such that

$$\mathbf{\Phi}_i = \begin{pmatrix} \mathbf{\Phi}_{i-1} & \mathbf{0} \\ -\mathbf{V}^T_{i-1,i}\mathbf{\Sigma}^{-1}_{i-1,i-1} & 1 \end{pmatrix} \text{ with } \mathbf{\Phi}_1 = \begin{pmatrix} 1 & 0 \\ -\sigma_{12}\sigma^{-1}_{11} & 1 \end{pmatrix},$$

and $\mathbf{D}_i$ is a diagonal matrix of $(d^2_{i-S_{X^*,i-1}}, \ldots, d^2_i)$ with $d^2_i = \sigma_{ii} - \mathbf{V}^T_{i-1,i}\mathbf{\Sigma}^{-1}_{i-1,i-1}\mathbf{V}_{i-1,i}$. Then, the transformed observation at time i is defined to be

$$X^*_i = \frac{X_i - \mu - \mathbf{V}^T_{i-1,i}\mathbf{\Sigma}^{-1}_{i-1,i-1}\mathbf{Z}_{i-1}}{d_i}, \qquad \text{for } i \geq 2,$$

and $\{X^*_{i-S_{X^*,i-1}}, \ldots, X^*_i\}$ is a series of decorrelated observations each of which has mean 0 and variance 1. In the above data decorrelation process, most computation is involved in

calculating $\mathbf{\Sigma}_{i-1,i-1}^{-1}$. To reduce the computing burden, Li and Qiu (2016) suggested using the following Woodbury formula for recursive computation:

$$\mathbf{\Sigma}_{i-1,i-1}^{-1} = \begin{pmatrix} \mathbf{\Sigma}_{i-2,i-2}^{-1} + \mathbf{\Sigma}_{i-2,i-2}^{-1}\mathbf{V}_{i-2,i-1}d_{i-1}^{-2}\mathbf{V}_{i-2,i-1}^{T}\mathbf{\Sigma}_{i-2,i-2}^{-1} & -\mathbf{\Sigma}_{i-2,i-2}^{-1}\mathbf{V}_{i-2,i-1}d_{i-1}^{-2} \\ -d_{i-1}^{-2}\mathbf{V}_{i-2,i-1}^{T}\mathbf{\Sigma}_{i-2,i-2}^{-1} & d_{i-1}^{-2} \end{pmatrix}.$$

You and Qiu (2019) suggested an alternative data decorrelation algorithm, which was shown faster than the algorithm described above.

The charting statistic of the proposed modified EWMA chart is then defined to be

$$E_{X^*,i}^{+} = \max\left\{0, \lambda X_i^* + (1-\lambda)E_{X^*,i-1}^{+} - k\right\}, \tag{6}$$

where λ and k are similar to those in Equation (3). If $E_{X^*,i}^{+} = 0$, then define $S_{X^*,i} = 0$. Otherwise, define $S_{X^*,i} = S_{X^*,i-1} + 1$.

The proposed modified EWMA chart with the charting statistic defined in Equations (5) and (6) gives a signal of an upward mean shift when

$$E_{X^*,i}^{+} > \rho, \qquad \text{for } i \geq 1, \tag{7}$$

where $\rho > 0$ is a control limit. Control charts for detecting downward or arbitrary mean shifts can be constructed similarly.

2.2 Monitoring Processes with Unequally Spaced Observation Times

In Section 2.1, observation times are assumed to be equally spaced, which is the default assumption in the conventional SPC literature. In practice, observation times could be unequally spaced (e.g., times of clinic visits of a patient). To monitor a process with unequally spaced observation times, the proposed EWMA chart can be modified easily to incorporate that feature of the observation times. Specifically, let $\{X_i, i \geq 1\}$ be the process to monitor with the observation times $\{t_i, i \geq 1\}$. Define $\omega > 0$ to be a basic time unit (Qiu 2024, Chapter 4) that all observation times $\{t_i, i \geq 1\}$

are its integer multiples. Then, we have $\{t_i = n_i\omega, \text{for } i \geq 1\}$, where n_i is the ith observation time in the basic time unit ω. At the current time point t_i, the charting statistic of the modified version of the EWMA chart is defined to be

$$E^+_{X^*,i} = \max\left\{0, \Lambda(t_i)X^*_i + (1-\Lambda(t_i))E^+_{X^*,i-1} - k\right\}, \tag{8}$$

where $E^+_{X^*,0} = 0$, $\Lambda(t_1) = 1-(1-\lambda)^{\overline{\Delta}}$, $\overline{\Delta} = \mathbb{E}(\Delta_i)$, $\Delta_i = n_i - n_{i-1}$, λ and k are tuning parameters similar to those in Equation (3), and

$$\Lambda(t_i) = \frac{\Lambda(t_{i-1})}{(1-\lambda)^{\Delta_i} + \Lambda(t_{i-1})}, \text{ for } i \geq 2.$$

The chart gives a signal of an upward mean shift when

$$E^+_{X^*,i} > \rho, \tag{9}$$

where $\rho > 0$ is a control limit. Here, $\{X^*_i, i \geq 1\}$ are obtained recursively through a standardization and decorrelation procedure similar to the one discussed in Section 2.1, where the restarting mechanism of $E^+_{X^*,i}$ affects the update of the sprint length $S_{X^*,i}$ and X^*_i. In the special case when $t_i = i$ for all $i \geq 1$ and $\omega = 1$, it can be checked that the control chart (8)-(9) is the same as the control chart (5)-(7).

In comparison, it is quite difficult to make modifications similar to the one described above for a CUSUM chart to accommodate unequally spaced observation times. In Section 3.3, it will be shown numerically that the proposed chart (8)-(9) could be more effective than a one-sided CUSUM chart for monitoring the standardized and decorrelated process observations in detecting upward mean shifts when observation times are unequally spaced.

As discussed in Qiu and Xiang (2014), the commonly used performance measure ARL would be inappropriate to use when the observation times are unequally spaced. The average time to signal (ATS) in the basic time unit of ω should be more appropriate to use in such cases.

2.3 Control Limit Determination

In the control chart (5)-(7), the smoothing parameter λ and the allowance parameter k are usually pre-specified but the control limit ρ should be chosen properly to reach a pre-specified ARL_0 or IC ATS (ATS_0) level. To this end, because the restarting mechanism is used in the construction of the chart and the current observation is decorrelated with all observations within the sprint length of the current observation time only, the control limit obtained for the conventional EWMA chart (1)-(2) cannot be used here. Instead, it should be computed in advance using Monte Carlo simulations. For all numerical examples presented in Section 3, it is determined in the following way. Using cases with equally spaced observation times as an example, for a given ρ value, we run $10,000$ replicated simulations of online process monitoring by the chart (5)-(7). For each simulation run, the run length value is recorded. Then, the ARL_0 value is estimated by the sample mean of the $10,000$ run length values. The control limit ρ can then be searched by a bisection algorithm or an alternative stochastic searching algorithm, as discussed in Capizzi and Masarotto (2016), so that the pre-specified ARL_0 level is achieved. For cases with unequally-spaced observation times, the control limit can be chosen in a similar way based on simulations of online process monitoring by the chart (8)-(9).

Obviously, the proposed control charts (5)-(7) and (8)-(9) can be used similarly in cases when the IC distribution is unknown and some IC parameters need to be estimated from an IC data. For example, as shown in Qiu et al. (2020) and Li and Qiu (2020), moment estimation can be used to estimate the IC mean, variance, and correlations, and the control limit of the related chart can be determined from the IC data by a bootstrap procedure. In addition, the self-starting version of the proposed control chart can be constructed in a similar way as that discussed in Li and Qiu (2020).

3 Simulation Studies

In this section, we first evaluate the numerical performance of the proposed modified EWMA chart (5)-(7) for online process monitoring of correlated data with equally spaced observation times. For the chart (5)-(7), we consider two versions. The first version is the one when k is chosen to be 0 so that the resulting chart only involves the weighting parameter λ and the control limit ρ and becomes much more convenient to use. This version is denoted as EWMA-RS1, where "RS" denotes "restarting". The second version allows a positive value for k and is denoted as EWMA-RS2. This version is more complex than EWMA-RS1 since one more procedure parameter k should be specified in its chart design. For comparison purposes, the conventional EWMA chart (1)-(2) that is applied to the original observed data is considered, which is denoted as EWMA-OR, where "OR" denotes "original". The one-sided EWMA chart (3)-(4) with $k = 0$ that is applied to the original observed data is also considered and denoted as EWMA-RSOR. In cases when the observed data are serially correlated, these charts have been shown to be unreliable (cf., Qiu 2014, Chapter 5). Another competing chart considered in this section is the conventional EWMA chart (1)-(2) that is applied to the fully decorrelated data (i.e., the current observation is decorrelated with all previous observations), which is denoted as EWMA-FD. This chart should be the most effective one among the five charts described above, but its computing burden would be heavy. Additionally, we consider two alternative approaches for monitoring serially correlated data: The first approach is the modified EWMA chart suggested by Zhang (1998) denoted as EWMA-Z, which accounts for the data autocorrelation by adjusting the control limits. This control chart assumes stationary autocorrelation in the process observations. While the charting statistics of EWMA-Z is updated in the same way as EWMA-OR, the chart gives a signal when $E_{X,i} > \sigma_E \rho_1$, where

$$\sigma_E^2 = \gamma(0) \times \left[1 + 2 \sum_{j=1}^{M} \frac{\gamma(j)}{\gamma(0)} (1-\lambda)^i \{ 1 - (1-\lambda)^{2(M-j)} \} \right],$$

$\gamma(j) = \text{cov}(X_i, X_{i+j})$ for $i \geq 1$ and $0 \leq j \leq M$, and $M > 0$ is a pre-specified integer and chosen to be 25 through the simulation studies as suggested by the author. The second approach is a residual-based chart, denoted as EWMA-AR(1). Particularly, it is assumed that the observed data follow the AR(1) model with mean 0, variance 1, and autoregressive coefficient 0.5. Based on these assumptions, the residuals of the AR(1) model can be computed, and the EWMA-OR chart is then applied to the computed residuals for online process monitoring.

The following six cases are considered in the simulation studies regarding the serial data correlation:

- **Case 1** IC process observations are i.i.d. with the IC process distribution $N(0, 1)$.
- **Case 2** IC process observations follow the AR(1) model $X_i = 0.5X_{i-1} + \varepsilon_i$, for $i \geq 1$, where $X_0 = 0$ and $\{\varepsilon_i\}$ are i.i.d. with the common distribution $N(0, 1)$.
- **Case 3** IC process observations follow the AR(1) model $X_i = 0.8X_{i-1} + \varepsilon_i$, for $i \geq 1$, where $X_0 = 0$ and $\{\varepsilon_i\}$ are i.i.d. with the common distribution $N(0, 1)$.
- **Case 4** IC process observations follow the MA(2) model $X_0 = 0$, $X_1 = \varepsilon_1$, $X_2 = \varepsilon_2 + 0.5\varepsilon_1$ and $X_i = \varepsilon_i + 0.5\varepsilon_{i-1} + 0.5\varepsilon_{i-2}$, for $i \geq 3$, where $\{\varepsilon_i\}$ are i.i.d. with the common distribution $N(0, 1)$.
- **Case 5** IC process observations follow the ARMA(2,1) model $X_i = 0.3X_{i-1} + 0.2X_{i-2} + 0.2\varepsilon_{i-1} + \varepsilon_i$, for $i \geq 2$, where $X_0 = X_1 = 0$ and $\{\varepsilon_i\}$ are i.i.d. with the common distribution $N(0, 1)$.
- **Case 6** IC process observations follow the model $X_i = 0.5Y_i + \varepsilon_i$, for $i \geq 1$, where $\{\varepsilon_i\}$ are i.i.d. with the common distribution $N(0, 1)$, and $\{Y_i, i \geq 1\}$ is a two-state Markov point

process with the states $\{0, 1\}$, the initial state 0, and the transition matrix

$$\begin{pmatrix} 0.8 & 0.2 \\ 0.2 & 0.8 \end{pmatrix}.$$

In each of the above 6 cases, IC process observations are always standardized to have the IC process mean 0 and IC process standard deviation 1. It can be seen that Case 1 represents the scenario in which all the model assumptions required by the conventional EWMA charts (1)-(2) are satisfied. Process observations in Cases 2 and 3 contain intermediate and strong serial data correlation, respectively, through the AR(1) models. Process observations in Case 4 contains short-range serial data correlation introduced by the MA(2) model. Serial data correlation in Case 5 is more complicated than that in Cases 2 to 4, and the one in Case 6 cannot be described by a conventional time series model.

3.1 IC performance and computing time

We first compare the IC performance of the seven control charts EWMA-RS1, EWMA-RS2, EWMA-OR, EWMA-RSOR, EWMA-Z, EWMA-AR(1), and EWMA-FD in different cases of serial data correlation. In the comparison, the nominal ARL_0 is fixed at 200 for each chart. The actual ARL_0 of each chart is computed as follows. First, the ARL_0 value is calculated by averaging the run length values obtained from $10,000$ replicated simulation runs of online process monitoring. In each simulation run, a total of $2,000$ process observations are monitored. If a given chart does not give any signal in a simulation run, then that run would be discarded when computing the ARL_0 value. In different cases considered, only less than 1% processes were actually discarded because of no signals by the 2,000th process observation. Thus, it should be sufficient for the simulation studies to specify the maximum run length to be $2,000$, which is 10 times the nominal ARL_0 value. Table 1 presents the calculated actual ARL_0 values and their standard errors (in parentheses) of the seven charts in all cases considered. The smoothing parameter λ in all charts is set to be the same

and takes the value in $\{0.05, 0.1, 0.2, 0.5\}$. The allowance constant k in EWMA-RS2 takes the value of 0.005 or 0.01. From the table, it can be seen that the charts EWMA-OR and EWMA-RSOR have reliable IC performances in Case 1 only, and their actual ARL_0 values in all other cases are quite far away from the nominal ARL_0 value of 200 as expected, since they ignores the serial correlation in these cases. EWMA-Z has reliable IC performance in Cases 1 and 6 only when no or weak serial data correlation is present. EWMA-AR(1) has reliable IC performance in Cases 2 and 4 only when the assumed time series model is either correct or close to the true model. As a comparison, all the other three charts EWMA-FD, EWMA-RS1 and EWMA-RS2 have reliable IC performances in all cases considered, since they all handle the serial data correlation properly in online process monitoring. The control limits of the control charts in all cases considered in Table 1 are presented in Table A.1 in the appendix. Table A.2 in the appendix presents the calculated actual ARL_0 values of EWMA-RS2 when k take the value in $\{0.05, 0.1, 0.2, 0.5\}$. It can be seen from that table that EWMA-RS2 has a reliable IC performance in those cases as well.

Next, we compare the computing time of the charts EWMA-FD, EWMA-RS1 and EWMA-RS2 in Cases 2-6 when process observations are serially correlated. The charts EWMA-OR, EWMA-RSOR, EWMA-Z and EWMA-AR(1) are excluded here since their actual ARL_0 values are substantially smaller or greater than the nominal ARL_0 value of 200 in these cases and thus their computing times are not comparable with those of the other three charts. The computing times of the charts EWMA-FD, EWMA-RS1 and EWMA-RS2 for computing their ARL_0 values, scaled by the function $\log(x+1)$, are presented in Figure 1. The original computing times are also presented in Table A.3 in Appendix. From the figure and the table, it can be seen that the proposed EWMA chart (5)-(7) takes dramatically less computing time compared to the EWMA-FD chart that decorrelates the process observation at the current time point with all previous observations. Therefore, the restarting mechanism introduced to this chart does help reduce the computing time. Note that EWMA-RS1 is the same as EWMA-RS2 when $k = 0$. From Figure 1 and Table A.3, it can be

Table 1: Calculated actual ARL_0 values and their standard errors (in the parentheses) of different control charts under different cases of serial data correlation. The nominal ARL_0 value of each chart is 200.

Cases	λ	EWMA-OR	EWMA-RSOR	EWMA-Z	EWMA-AR(1)	EWMA-FD	EWMA-RS1	EWMA-RS2	
								$k = 0.005$	$k = 0.01$
1	0.05	201.09 (1.98)	200.69 (1.88)	201.09 (1.98)	704.05 (5.25)	201.09 (1.98)	200.69 (1.88)	201.02 (1.93)	199.83 (1.95)
	0.10	198.98 (1.94)	197.51 (1.91)	198.98 (1.94)	758.11 (5.42)	198.98 (1.94)	197.51 (1.91)	199.27 (1.94)	198.40 (1.93)
	0.20	197.24 (1.95)	201.91 (2.00)	197.24 (1.95)	639.84 (5.05)	197.24 (1.95)	201.91 (2.00)	201.53 (2.00)	200.66 (1.99)
	0.50	201.47 (2.01)	197.94 (1.97)	201.47 (2.01)	178.66 (1.78)	201.47 (2.01)	197.94 (1.97)	198.42 (1.97)	198.07 (1.96)
2	0.05	80.40 (0.82)	63.08 (0.56)	234.66 (2.27)	201.09 (1.98)	201.55 (1.98)	201.70 (1.90)	199.56 (1.91)	199.20 (1.97)
	0.10	67.49 (0.66)	57.06 (0.52)	277.33 (2.67)	198.98 (1.94)	199.31 (1.94)	199.21 (1.93)	198.31 (1.94)	197.15 (1.92)
	0.20	61.18 (0.60)	57.82 (0.55)	293.77 (2.87)	197.24 (1.95)	197.38 (1.95)	198.56 (1.95)	197.76 (1.95)	197.28 (1.95)
	0.50	76.23 (0.75)	82.89 (0.83)	281.28 (2.73)	201.47 (2.01)	201.88 (2.01)	201.61 (2.01)	201.98 (2.02)	201.44 (2.01)
3	0.05	62.42 (0.67)	49.60 (0.45)	303.47 (2.86)	112.50 (1.12)	201.95 (1.98)	202.91 (1.93)	200.28 (1.93)	199.86 (1.96)
	0.10	52.87 (0.53)	47.67 (0.44)	402.43 (3.70)	110.12 (1.06)	200.00 (1.94)	199.32 (1.93)	200.50 (1.95)	198.52 (1.95)
	0.20	50.70 (0.49)	51.37 (0.49)	448.17 (4.03)	129.04 (1.26)	198.27 (1.95)	197.74 (1.96)	196.91 (1.97)	196.13 (1.96)
	0.50	75.57 (0.74)	83.92 (0.82)	436.13 (3.98)	307.96 (2.99)	202.10 (2.01)	201.38 (2.01)	201.61 (2.01)	202.26 (2.02)
4	0.05	83.13 (0.85)	64.22 (0.57)	226.57 (2.21)	221.25 (2.18)	201.50 (1.98)	201.36 (1.91)	200.62 (1.92)	199.00 (1.95)
	0.10	69.08 (0.68)	57.20 (0.52)	263.09 (2.55)	217.33 (2.13)	199.33 (1.94)	199.60 (1.94)	198.89 (1.94)	198.77 (1.95)
	0.20	61.26 (0.60)	56.56 (0.53)	281.73 (2.76)	208.33 (2.08)	197.48 (1.95)	198.65 (1.95)	199.17 (1.95)	199.64 (1.96)
	0.50	73.69 (0.72)	79.37 (0.78)	280.76 (2.76)	204.57 (2.05)	201.89 (2.01)	201.73 (2.01)	201.90 (2.01)	201.36 (2.01)
5	0.05	75.52 (0.77)	59.54 (0.51)	257.57 (2.49)	162.81 (1.60)	204.02 (2.01)	199.96 (1.88)	199.26 (1.89)	198.37 (1.91)
	0.10	64.14 (0.62)	55.08 (0.48)	312.12 (2.97)	160.68 (1.53)	202.21 (1.96)	197.08 (1.90)	197.29 (1.90)	196.37 (1.88)
	0.20	58.15 (0.54)	56.84 (0.52)	331.65 (3.12)	167.24 (1.62)	199.52 (1.92)	197.99 (1.90)	197.64 (1.89)	196.88 (1.88)
	0.50	75.89 (0.72)	83.42 (0.79)	311.20 (2.95)	217.85 (2.13)	205.83 (2.00)	198.96 (1.93)	198.58 (1.92)	198.37 (1.92)
6	0.05	173.66 (1.72)	164.11 (1.51)	201.65 (1.99)	621.33 (4.92)	198.70 (1.96)	203.15 (1.90)	202.49 (1.91)	204.47 (1.96)
	0.10	167.12 (1.64)	160.74 (1.53)	203.47 (1.97)	682.23 (5.17)	196.39 (1.91)	205.16 (1.94)	203.46 (1.94)	204.31 (1.95)
	0.20	165.16 (1.60)	166.71 (1.61)	205.69 (1.99)	581.10 (4.76)	198.33 (1.93)	203.07 (1.97)	203.77 (1.98)	204.53 (1.99)
	0.50	179.27 (1.78)	181.11 (1.77)	208.51 (2.05)	181.08 (1.80)	203.91 (2.01)	199.76 (1.95)	203.10 (1.99)	202.89 (1.99)

seen that the computing time of EWMA-RS2 is generally shorter when k is chosen larger, which is intuitively reasonable because the charting statistics would be reset to 0 more frequently when k is larger. Thus, the sprint length would be shorter which leads to less data decorrelation. It can also be seen from the figure that some computing times are missing in the plot when λ is small and k is chosen relatively large. Based on extensive numerical studies, we find that the pre-specified ARL_0 cannot be achieved in these cases for the following reason. While λ controls the variability of the charting statistics and k is related to a target shift, the charting statistics would be difficult to exceed a control limit when λ is small (or the charting statistic has a small variability) and k is chosen large since the charting statistics are reset to 0 too often in such cases. In addition, the figure suggests that the computing times of different charts do not change much in Cases 2-6.

3.2 Out-of-Control (OC) performance

Next, we study the OC performance of the seven related control charts in Cases 1-6. In each case, a mean shift of size δ is assumed to occur at the 51st time points, and δ can change among $\{0.3, 0.6, 0.9, 1.2, 1.5\}$. Then, the OC ARL ($ARL_1$) values of the charts are computed in the same way as their ARL_0 values, except that a simulation run with a signal before the occurrence of the mean shift would be skipped in computing the related ARL_1 value. To make the comparison fair, the control limits of all charts have been adjusted properly so that their actual ARL_0 values are all equal to 200. In addition, for detecting a given shift, the minimum (or optimal) ARL_1 values of the charts are computed by changing their procedure parameter values. Otherwise, their ARL_1 values may not be comparable when their procedure parameters are pre-specified (Qiu, 2008). To compute the optimal ARL_1 value of the chart EWMA-RS2 in a given case, the Nelder-Mead algorithm with constraints (Luersen et al., 2004) should be helpful when searching for the minimum ARL_1 value when both parameters λ and k change.

Table 2 presents the optimal ARL_1 values of the seven charts in Cases 1-6 in the natural log

Figure 1: Computing times of the charts EWMA-FD, EWMA-RS1 and EWMA-RS2 for computing their ARL_0 values in Cases 2-6 with different choices of λ and k. The vertical axis is scaled by the function $\log(x+1)$.

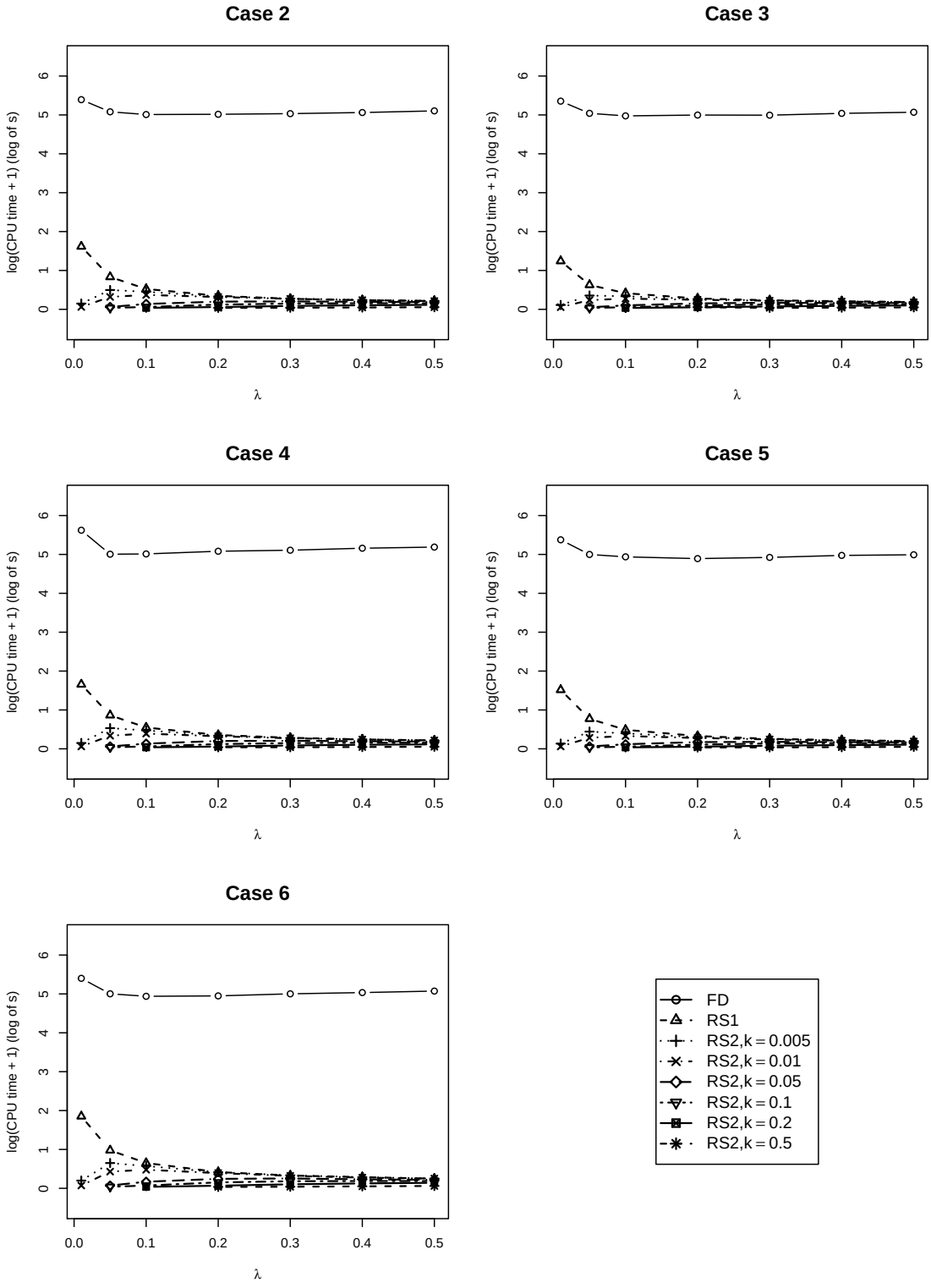

scale. From the plots in the figure, we can have the following conclusions. i) In all cases considered, the EWMA-OR, EWMA-Z, EWMA-AR(1) and EWMA-FD charts have very similar performance while the EWMA-RSOR and EWMA-RS1 charts have very similar performance. However, from Table 1, the charts EWMA-OR, EWMA-RSOR, EWMA-Z and EWMA-AR(1) would not be reliable to use in Cases 2-6 when there exists different types of serial data correlation. ii) In all cases considered, either EWMA-FD or EWMA-RS2 has the smallest optimal ARL_1 values for detecting most of the mean shift δ. EWMA-RS2 usually slightly outperforms other charts for detecting moderate to large mean shift. iii) The difference among the charts EWMA-RS1, EWMA-RS2 and EWMA-FD is small in all cases considered, especially in Case 1 when the IC process observations are i.i.d. and normally distributed. In Cases 2-6 when serial data correlation is present, the charts EWMA-RS1 and EWMA-RS2 have a slightly worse performance compared to the chart EWMA-FD for detecting small to moderate mean shifts.

The optimal values of λ used in the chart EWMA-RS1 and the optimal values of λ and k used in the chart EWMA-RS2 in various cases considered in Table 2 are shown in Figure 2. From the plots in the figure, it can be seen that the optimal value of λ used in EWMA-RS1 increases when δ becomes larger, which is consistent with the guidelines for the design of the conventional EWMA charts (Crowder, 1989). For the two parameters λ and k used in EWMA-RS2, their optimal values have more complex relationships with the shift size δ, although they both have increasing trends with δ. From the figure, it seems that the optimal value of k used in EWMA-RS2 is close to 0 for detecting small shifts (e.g., $\delta \leq 0.5$).

The zero-state optimal ARL_1 values (i.e., the values when the mean shift is assumed to occur at the beginning of process monitoring) of the seven charts in all the cases considered in Table 2 are shown in Figure A.4 in Appendix. The related optimal values of λ used in EWMA-RS1 and the optimal values of λ and k used in EWMA-RS2 are shown in Figure A.2 in Appendix. Similar conclusions can be made from these results to those from the results in Table 2 and Figure 2.

Table 2: Calculated optimal ARL_1 values and their standard errors (in the parentheses) of different control charts under different cases of serial data correlation. The nominal ARL_0 value of each chart is 200. The smallest optimal ARL_1 value among the seven charts is highlighted in bold in each case considered.

Cases	δ	EWMA-OR	EWMA-RSOR	EWMA-Z	EWMA-AR(1)	EWMA-FD	EWMA-RS1	EWMA-RS2
1	0.3	**29.43** (0.22)	30.67 (0.23)	**29.43** (0.22)	29.64 (0.22)	**29.43** (0.22)	30.67 (0.23)	30.64 (0.23)
	0.6	13.43 (0.09)	13.27 (0.09)	13.43 (0.09)	13.89 (0.09)	13.43 (0.09)	13.27 (0.09)	**13.25** (0.09)
	0.9	7.90 (0.05)	7.77 (0.05)	7.90 (0.05)	8.35 (0.05)	7.90 (0.05)	7.77 (0.05)	**7.76** (0.05)
	1.2	5.29 (0.03)	5.19 (0.03)	5.29 (0.03)	5.67 (0.03)	5.29 (0.03)	5.19 (0.03)	**5.18** (0.03)
	1.5	3.88 (0.02)	3.80 (0.02)	3.88 (0.02)	4.15 (0.02)	3.88 (0.02)	3.80 (0.02)	**3.77** (0.02)
2	0.3	47.96 (0.40)	52.79 (0.44)	47.96 (0.40)	47.67 (0.40)	**47.60** (0.40)	53.94 (0.44)	53.95 (0.44)
	0.6	24.91 (0.18)	25.18 (0.19)	24.91 (0.18)	24.86 (0.18)	**24.85** (0.18)	25.89 (0.20)	25.88 (0.20)
	0.9	15.05 (0.11)	**14.90** (0.11)	15.05 (0.11)	15.02 (0.11)	15.04 (0.11)	15.31 (0.11)	15.03 (0.11)
	1.2	10.09 (0.07)	**10.01** (0.07)	10.09 (0.07)	10.07 (0.07)	10.07 (0.07)	10.23 (0.08)	**10.01** (0.07)
	1.5	7.19 (0.05)	7.08 (0.05)	7.19 (0.05)	7.20 (0.05)	7.20 (0.05)	7.23 (0.05)	**6.99** (0.05)
3	0.3	73.68 (0.69)	81.75 (0.75)	73.68 (0.69)	73.24 (0.69)	**72.69** (0.69)	82.97 (0.77)	82.99 (0.78)
	0.6	40.22 (0.34)	43.94 (0.37)	40.22 (0.34)	39.83 (0.33)	**39.30** (0.33)	44.34 (0.39)	44.55 (0.39)
	0.9	27.01 (0.23)	27.24 (0.22)	27.01 (0.23)	26.67 (0.22)	**25.82** (0.21)	27.62 (0.24)	27.37 (0.24)
	1.2	18.09 (0.15)	18.18 (0.15)	18.09 (0.15)	17.98 (0.15)	**17.85** (0.15)	18.23 (0.16)	18.18 (0.16)
	1.5	12.74 (0.12)	12.71 (0.12)	12.74 (0.12)	12.66 (0.12)	**12.52** (0.12)	12.72 (0.12)	12.72 (0.12)
4	0.3	45.67 (0.37)	50.29 (0.41)	45.68 (0.37)	45.46 (0.37)	**45.45** (0.37)	51.14 (0.41)	51.12 (0.41)
	0.6	23.49 (0.17)	23.71 (0.17)	23.49 (0.17)	**23.35** (0.17)	23.43 (0.17)	24.53 (0.19)	24.50 (0.19)
	0.9	14.18 (0.10)	**14.11** (0.10)	14.18 (0.10)	14.25 (0.10)	14.20 (0.10)	14.45 (0.10)	14.25 (0.10)
	1.2	9.57 (0.07)	9.52 (0.07)	9.57 (0.07)	9.59 (0.07)	9.48 (0.07)	9.68 (0.07)	**9.47** (0.07)
	1.5	6.89 (0.05)	6.79 (0.05)	6.89 (0.05)	6.88 (0.05)	6.82 (0.05)	6.84 (0.05)	**6.67** (0.05)
5	0.3	53.54 (0.47)	59.93 (0.52)	53.54 (0.47)	53.16 (0.47)	**52.87** (0.46)	60.80 (0.52)	60.78 (0.52)
	0.6	28.87 (0.22)	29.32 (0.23)	28.87 (0.22)	**28.82** (0.22)	28.83 (0.22)	30.30 (0.23)	30.31 (0.23)
	0.9	17.69 (0.13)	**17.59** (0.13)	17.69 (0.13)	17.57 (0.13)	17.62 (0.13)	18.29 (0.14)	17.93 (0.14)
	1.2	11.80 (0.09)	11.70 (0.09)	11.80 (0.09)	11.73 (0.09)	11.79 (0.09)	12.00 (0.09)	**11.69** (0.09)
	1.5	8.33 (0.06)	8.23 (0.06)	8.33 (0.06)	8.31 (0.07)	8.33 (0.06)	8.41 (0.07)	**8.09** (0.06)
6	0.3	32.39 (0.24)	32.74 (0.25)	31.73 (0.24)	32.01 (0.24)	**31.41** (0.23)	34.24 (0.28)	34.26 (0.28)
	0.6	14.60 (0.10)	**14.57** (0.10)	**14.57** (0.10)	15.03 (0.10)	14.59 (0.10)	14.70 (0.10)	14.59 (0.10)
	0.9	8.48 (0.05)	8.37 (0.05)	8.51 (0.05)	8.85 (0.06)	8.51 (0.05)	8.41 (0.05)	**8.36** (0.05)
	1.2	5.63 (0.03)	5.54 (0.03)	5.70 (0.04)	6.03 (0.04)	5.66 (0.03)	5.55 (0.03)	**5.53** (0.03)
	1.5	4.11 (0.02)	4.02 (0.02)	4.09 (0.02)	4.42 (0.03)	4.12 (0.02)	4.03 (0.02)	**3.97** (0.02)

Figure 2: Optimal values of λ used in EWMA-RS1 and optimal values of λ and k used in EWMA-RS2 in various cases considered in Figure 2.

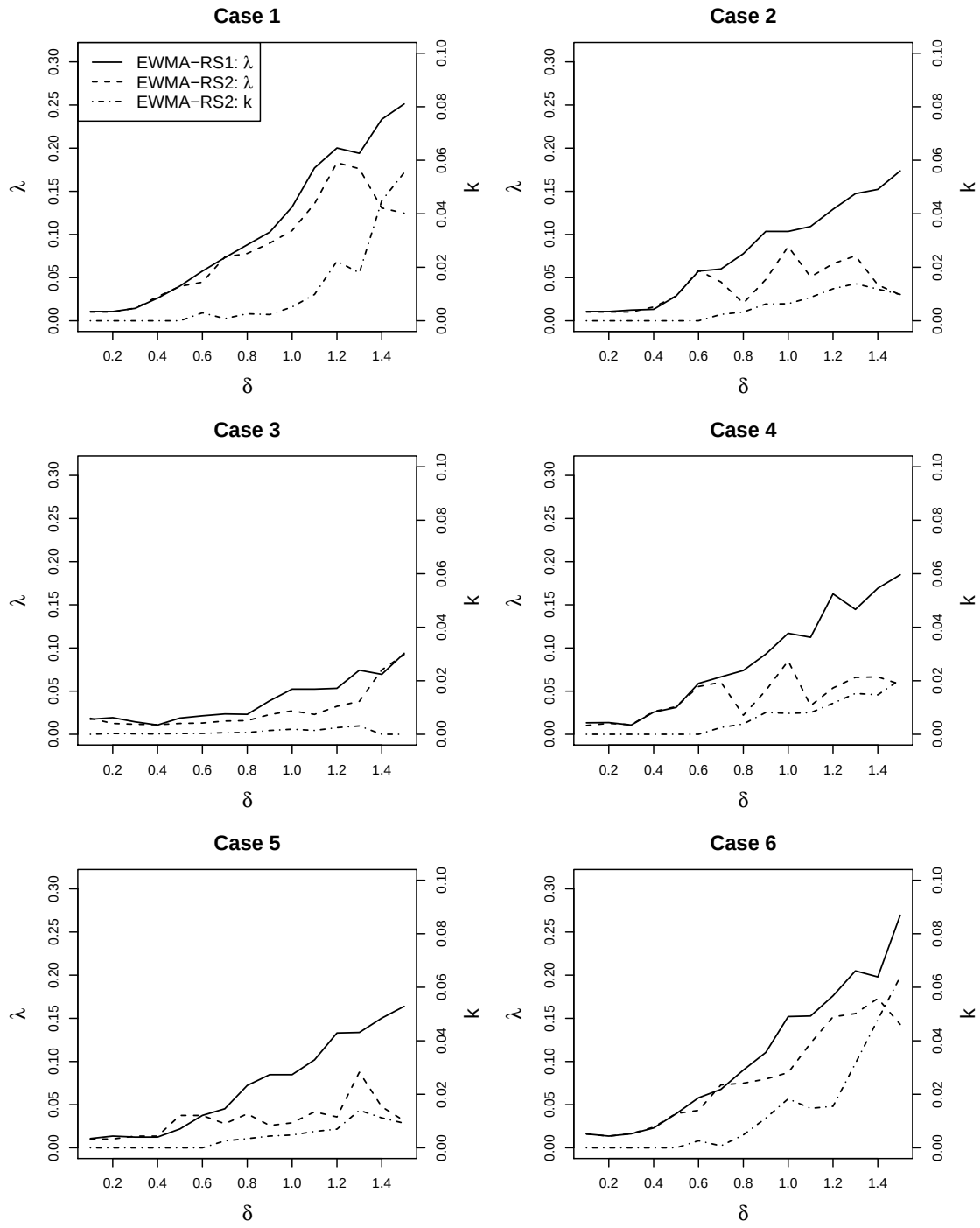

From the results presented in Sections 3.1 and 3.2, it can be seen that i) the charts EWMA-OR and EWMA-RSOR are unreliable to use when the observed data are serially correlated (cf., Table 1), ii) all the charts EWMA-FD, EWMA-RS1 and EWMA-RS2 are reliable when monitoring correlated data (cf., Table 1), but the computational demand of EWMA-FD is very heavy (cf., Figure 1), iii) the computational demands of EWMA-RS1 and EWMA-RS2 are much less than that of EWMA-FD (cf., Figure 1), and their OC performance is comparable to that of EWMA-FD (cf., Table 2), and iv) the OC performance of EWMA-RS1 and EWMA-RS2 is almost identical in all cases considered (cf., Table 2). Based on these results, we suggest using the chart EWMA-RS1 for monitoring correlated data in practice, because it has only one parameter λ to choose while EWMA-RS2 has two parameters λ and k to choose.

3.3 Comparison with the CUSUM chart

In this subsection, we further compare the proposed control charts EWMA-RS1 and EWMA-RS2 with the one-sided version of the CUSUM chart discussed in Qiu et al. (2020) for monitoring correlated data, which is denoted as CUSUM-RS. Specifically, the charting statistic of CUSUM-RS is defined to be

$$C^+_{X^*,i} = \max\left\{0, X^*_i + C^+_{X^*,i-1} - k\right\},$$

where k is the allowance parameter, $C_{X^*,0} = 0$, and $\{X^*_i, i \geq 1\}$ are the standardized and decorrelated process observations obtained by a procedure similar to the one discussed in Section 2.1. The CUSUM-RS chart gives a signal of an upward mean shift when $C^+_{X^*,i} > h$, where $h > 0$ is a control limit chosen by a Monte Carlo procedure similar to the one described in Section 2.3.

Observation times $\{t_i, i \geq 1\}$ are assumed to be within the design interval $[0, 2, 000]$. The following two settings of observation times are considered: (i) observation times are just $\{1, 2, \ldots, 2000\}$ (i.e., they are equally spaced); and (ii) observation times are defined recursively by $t_{i+1} = t_i + W_i$, for $i \geq 1$, until t_i exceeds 2000, where $W_i = 1$ for $1 \leq i \leq 10$, $W_i = 2$ for $11 \leq i \leq 20$,

$\ldots$, $W_i = k$ for $10(k-1)+1 \le i \le 10k$. Thus, observation times are unequally spaced in the second setting. Process observations are generated as discussed at the beginning of Section 3 in Cases 1-3. Namely, they are i.i.d. and $N(0,1)$ distributed in Case 1, and follow the AR(1) model with the parameter value to be 0.5 and 0.8, respectively, in Cases 2 and 3. With the basic time unit chosen to be $\omega = 1$, the actual ATS values of the related charts are computed in a way similar to that for computing the ARL values in Sections 3.1 and 3.2. For all the charts, their nominal ATS_0 values are fixed at 200. By the way, in Setting (ii) when the observation times are unequally spaced, EWMA-RS1 and EWMA-RS2 are constructed as discussed in Section 2.2.

Tables A.5 and A.6 in Appendix present the calculated actual ATS_0 values and their standard errors of the control charts CUSUM-RS, EWMA-RS1 and EWMA-RS2 in the two different settings of the observation times, respectively, when the allowance constant k in CUSUM-RS is chosen to be one of $\{0.25, 0.5, 0.75, 1\}$ and the parameters λ and k in EWMA-RS1 and EWMA-RS2 are chosen in the same way as that in Table 1 and Table A.2. From the tables, it can be seen that all three charts have reliable IC performance in all cases considered. The average computing times of the three charts for computing their corresponding ATS_0 values are presented in Tables A.7 and A.8 in Appendix, from which it can be seen that their computing times are comparable as well in all cases considered.

Next, we compare the OC performance of the related charts. Table 3 presents their optimal zero-state ATS_1 values for both settings of the observation times in cases when the process mean has a shift of size δ that changes among $\{0.3, 0.6, 0.9, 1.2, 1.5\}$ and the nominal ATS_0 value is set to be 200 for all charts. Here, only the zero-state ATS_1 is considered because the presence of unequally spaced observation times prevents the distribution of the charting statistic of a given chart from being stable after a given number (e.g., 50) of basic time units. From the table, it can be seen that CUSUM-RS performs the best in all cases of Setting (i) when the observation times are equally spaced. However, in Setting (ii) when the observation times are unequally spaced, both EWMA-

RS1 and EWMA-RS2 outperforms CUSUM-RS in cases considered, because the former two charts have taken into account the unequally spaced observation times in their chart construction while the latter chart has not. For EWMA-RS1 and EWMA-RS2, their optimal choices of λ and k in Setting (ii) have similar patterns to those shown in Figure 3 and Figure A.2, and thus are omitted here. In addition, in Setting (ii) when the observation times are unequally spaced, it seems that EWMA-RS2 outperforms EWMA-RS1 for detecting intermediate to large shifts (e.g., $\delta \geq 0.9$) because the former employs one more parameter (i.e., k) in its charting statistic than the latter.

Table 3: Optimal zero-state ATS_1 values and their standard errors (in the parentheses) of the charts CUSUM-RS, EWMA-RS1 and EWMA-RS2 for both settings of the observation times in cases when the process mean has a shift of size δ that changes among $\{0.3, 0.6, 0.9, 1.2, 1.5\}$ and the nominal ATS_0 value is set to be 200 for all charts. The smallest optimal ATS_1 value among the three charts is highlighted in bold in each case considered.

		Setting (i)			Setting (ii)		
Cases	δ	CUSUM-RS	EWMA-RS1	EWMA-RS2	CUSUM-RS	EWMA-RS1	EWMA-RS2
1	0.3	**35.56** (0.24)	36.01 (0.23)	36.01 (0.23)	29.87 (0.39)	**23.33** (0.39)	**23.33** (0.39)
	0.6	**15.04** (0.10)	15.388 (0.09)	15.076 (0.09)	10.422 (0.11)	7.412 (0.09)	**6.21** (0.10)
	0.9	**8.56** (0.05)	8.82 (0.05)	8.56 (0.05)	5.66 (0.04)	4.05 (0.04)	**3.12** (0.04)
	1.2	**5.61** (0.03)	5.894 (0.03)	5.61 (0.03)	3.84 (0.03)	2.71 (0.02)	**2.12** (0.02)
	1.5	**4.04** (0.02)	4.256 (0.02)	4.04 (0.02)	2.79 (0.02)	2.02 (0.01)	**1.63** (0.01)
2	0.3	**60.57** (0.47)	61.55 (0.45)	61.55 (0.45)	42.77 (0.46)	**35.58** (0.47)	**35.58** (0.47)
	0.6	**28.67** (0.21)	29.82 (0.20)	28.88 (0.21)	19.42 (0.17)	14.33 (0.17)	**12.82** (0.18)
	0.9	**16.79** (0.12)	17.59 (0.12)	16.80 (0.12)	11.05 (0.10)	7.63 (0.08)	**5.95** (0.09)
	1.2	**10.77** (0.07)	11.59 (0.08)	10.82 (0.08)	7.17 (0.06)	4.74 (0.06)	**3.32** (0.05)
	1.5	**7.41** (0.05)	8.16 (0.05)	7.43 (0.06)	4.99 (0.04)	3.09 (0.04)	**2.06** (0.03)
3	0.3	**90.41** (0.77)	92.11 (0.78)	92.11 (0.78)	66.39 (0.74)	**58.95** (0.78)	**58.95** (0.78)
	0.6	**49.77** (0.39)	50.86 (0.40)	50.86 (0.40)	33.22 (0.32)	26.69 (0.33)	**25.63** (0.40)
	0.9	**30.57** (0.24)	31.94 (0.25)	30.88 (0.26)	20.00 (0.20)	14.64 (0.18)	**12.07** (0.29)
	1.2	**20.40** (0.17)	21.83 (0.17)	20.52 (0.18)	13.04 (0.13)	8.76 (0.11)	**5.13** (0.14)
	1.5	**14.05** (0.13)	15.63 (0.12)	14.05 (0.15)	8.71 (0.09)	5.23 (0.08)	**2.48** (0.07)

4 Case Study

El Niño is a climate phenomenon characterized by the periodic warming of sea surface temperatures in the central and eastern equatorial Pacific Ocean. This natural phenomenon has far-reaching and often disruptive effects on weather patterns and ecosystems across the globe (Trenberth and Hoar, 1997). El Niño events typically occur every 2 to 7 years and can last for several months. When El Niño develops, it can lead to a variety of climate-related consequences, including altered precipitation patterns, more frequent and severe storms, droughts, and extreme temperatures. These impacts can have profound damage on agriculture, fisheries, water resources, and even human health (Glantz, 2001). El Niño events are closely monitored by meteorologists and climate scientists to better predict and prepare for their regional and global impacts. The Niño 3 region is a specific area in the equatorial Pacific Ocean that plays a critical role in monitoring and understanding El Niño and La Niña events. This region is defined by a specific set of coordinates, typically spanning 120W-170W and 5S-5N (Cane, 2005). In this section, we demonstrate the proposed control chart (5)-(7) using a dataset measuring the sea surface temperatures in the Niño 3 region.

The original source of the dataset is the Climate Prediction Center of the USA. It can also be obtained from the R package **tseries**. From January 1950 to October 1999, a total of 598 observations of sea surface temperature of the Niño 3 Region in degrees Celsius were measured monthly. We then split the data into two parts with the first 350 observations as the IC dataset and the remaining 248 observations for online process monitoring. The Sharpiro-Wilk test for normality of the IC data gives a p-value of 6.696×10^{-6}, indicating that the IC data are not normally distributed. To facilitate finding the control limits for the proposed control charts as discussed in Section 2, we use Johnson's transformation families (Johnson, 1949; Chou et al., 1998) to normalize the original observations. The transformed data are shown in Figure 3. From the figure, it can be seen that the IC data look quite stable while the remaining data seem to have an upward mean shift starting around

the 390th month, which matches the most powerful El Niño events in the recorded history that happened during 1982-1983 (i.e., between months 384-394) (Caviedes, 1984). Now, the Sharpiro-Wilk test for checking the normality of the transformed IC data gives a p-value of 0.146, implying that we fail to reject the normality of the transformed IC data. The Augmented Dickey-Fuller (ADF) test and the Phillips-Perron (PP) test for checking stationarity of the IC dataset both give p-values less than 0.01, indicating the stationarity assumption is not violated. Based on the autocorrelation function (ACF) plot of the IC data, the correlation between any two observations whose observation times are at least 30-month apart is negligible. Therefore, the IC mean, variance, and covariances $\text{cov}(X_i, X_{i-s})$, for any $i \geq 1$ and $s = 1, 2, \ldots, 30$, can be estimated from the IC data by the moment estimates, and the estimated IC parameters can be used in data decorrelation discussed in Section 2.

Figure 3: Transformed observations of the sea surface temperature dataset. The vertical dashed line separates the IC data of 350 observations from the remaining 248 observations for online process monitoring.

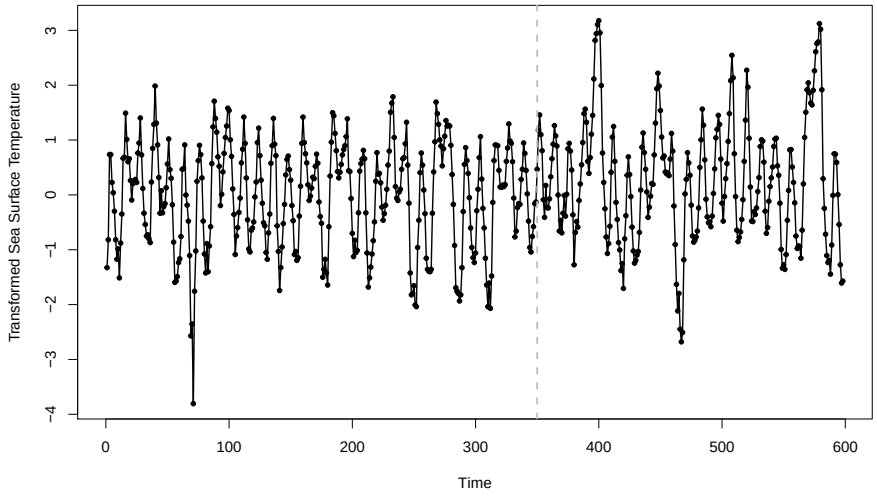

Then, the 8 control charts EWMA-OR, EWMA-RSOR, EWMA-Z, EWMA-AR(1), EWMA-FD, EWMA-RS1, EWMA-RS2, and CUSUM-RS are applied to the data for online process mon-

itoring starting from the 351th observation. The nominal ARL_0 is fixed at 200 for each control chart. The weighting parameters λ is chosen to be 0.1 in all EWMA type charts. The allowance parameter k in EWMA-RS2 and CUSUM-RS charts are chosen to be 0.01 and 0.1 respectively. Figure 4 shows the six control charts with the related control limits labeled by the dashed horizontal lines. From the plots, it can be seen that both EWMA-RS1 and EWMA-RS2 give their first signals at the 395th observation time. EWMA-OR and EWMA-RSOR give their first signals at the 365th and 366th observation times, respectively. From Figure 3, it can be seen that these could be false signals since there is no obvious shift before these time points. EWMA-Z and EWMA-AR(1) give their first signals at the 396th and 397th observations times, respectively. The chart EWMA-FD gives its first signal at the 394th observation time, and the chart CUSUM-RS gives its first signal at the 395th observation time. Collectively, the results from the charts EWMA-RS1, EWMA-RS2, EWMA-FD and CUSUM-RS are similar, but the chart EWMA-FD is the slowest to compute.

5 Concluding Remarks

Since the observed data of most sequential processes in practice are serially correlated, control charts that can properly account for the serial data correlation are useful. In the previous sections, we have described the modified EWMA chart (5)-(7) that contains a restarting mechanism, and shown that it is fast to compute and reliable to use for monitoring correlated data without sacrificing much OC performance. Although this chart is introduced in simple cases for detecting upward mean shifts in a univariate process, its idea is general and can be used in other cases, such as the ones for detecting downward or arbitrary mean shifts in a univariate process. In practice, there could be multiple quality variables to monitor. In such cases, the computing time becomes a more important concern because the computational burden associated with the multivariate version of the data decorrelation procedure increases exponentially with the dimensionality of the process

observations. Therefore, it requires much future research to generalize the modified EWMA chart (5)-(7) to cases with multivariate serially correlated data.

Figure 4: Charting statistics of the eight control charts EWMA-OR, EWMA-RSOR, EWMA-Z, EWMA-AR(1), EWMA-FD, EWMA-RS1, EWMA-RS2, and CUSUM-RS for monitoring the transformed sea surface temperature data in the Niño 3 region. The dashed horizontal line in each plot denotes the control limit of the related control chart.

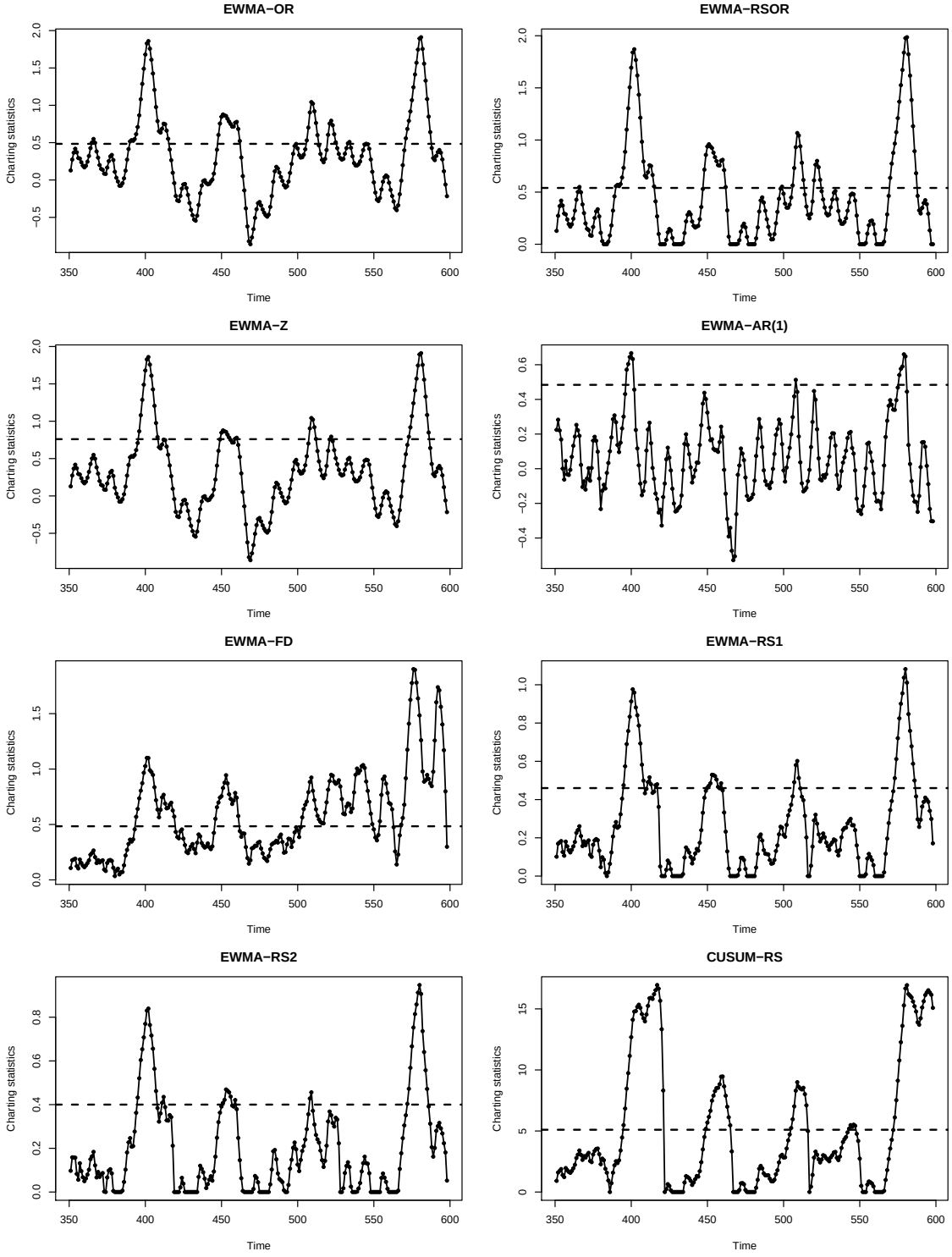

Appendix: Additional Numerical Results

Some additional numerical results mentioned in the main article are provided in this appendix. More specifically, corresponding to the choices of parameters and cases of serial data correlation shown in Table 1, Table A.1 includes the simulated control limits of different control charts so that the nominal ARL_0 can be achieved. Table A.2 presents the calculated actual ARL_0 values and standard errors of the EWMA-RS2 chart when k takes the value in $\{0.05, 0.1, 0.2, 0.5\}$. Table A.3 presents the average computing times (in seconds) of the charts EWMA-FD, EWMA-RS1, and EWMA-RS2 to compute their ARL_0 values. As discussed in the main article, EWMA-RS2 cannot give signals for some specific combinations of λ and k and the computation times are thus missing and denoted as "–" in the table. Table A.4 presents the optimal zero-state ARL_1 of the seven control charts in all cases considered in Table 2 of the main paper. Tables A.5 and A.6 present the calculated ATS_0 and the standard errors of the charts CUSUM-RS, EWMA-RS1 and EWMA-RS2 in Settings (i) and (ii) of the observation times. Tables A.7 and A.8 show the average computing times of the charts CUSUM-RS, EWMA-RS1 and EWMA-RS2 to compute their ARL_0 values. The corresponding optimal values of λ used in EWMA-RS1 and the optimal values of λ and k used in EWMA-RS2 are shown in Figure A.1.

Table A.1: Simulated control limits of different control charts in cases considered in Table 1.

Cases	λ	EWMA-OR	EWMA-RSOR	EWMA-FD	EWMA-RS1	EWMA-RS2	
						$k = 0.005$	$k = 0.01$
1	0.05	0.288	0.343	0.288	0.343	0.288	0.244
	0.10	0.484	0.541	0.484	0.541	0.508	0.477
	0.20	0.780	0.844	0.780	0.844	0.824	0.806
	0.50	1.463	1.523	1.463	1.523	1.516	1.507
2	0.05	0.288	0.343	0.288	0.327	0.269	0.224
	0.10	0.484	0.541	0.484	0.517	0.480	0.448
	0.20	0.780	0.844	0.780	0.802	0.781	0.761
	0.50	1.463	1.523	1.463	1.438	1.429	1.419
3	0.05	0.288	0.343	0.288	0.304	0.245	0.201
	0.10	0.484	0.541	0.484	0.484	0.447	0.414
	0.20	0.780	0.844	0.780	0.757	0.736	0.715
	0.50	1.463	1.523	1.463	1.381	1.371	1.361
4	0.05	0.288	0.343	0.288	0.330	0.273	0.228
	0.10	0.484	0.541	0.484	0.522	0.486	0.454
	0.20	0.780	0.844	0.780	0.811	0.791	0.772
	0.50	1.463	1.523	1.463	1.451	1.441	1.431
5	0.05	0.288	0.343	0.288	0.319	0.261	0.217
	0.10	0.484	0.541	0.484	0.505	0.470	0.436
	0.20	0.780	0.844	0.780	0.785	0.765	0.744
	0.50	1.463	1.523	1.463	1.402	1.392	1.383
6	0.05	0.288	0.343	0.288	0.344	0.288	0.244
	0.10	0.484	0.541	0.484	0.544	0.509	0.477
	0.20	0.780	0.844	0.780	0.841	0.822	0.804
	0.50	1.463	1.523	1.463	1.511	1.505	1.497

Table A.2: Calculated actual ARL_0 values and their standard deviations (in the parentheses) of EWMA-RS2 when λ and k take several different values. The nominal ARL_0 is fixed at 200. "–" in some entries imply that the actual ARL_0 values cannot be computed in the related cases as discussed in the main article.

Cases	λ	EWMA-RS2			
		$k = 0.05$	$k = 0.1$	$k = 0.2$	$k = 0.5$
1	0.05	199.14 (1.98)	204.57 (2.03)	–	–
	0.10	200.90 (1.99)	199.83 (1.98)	204.51 (2.03)	–
	0.20	199.75 (1.98)	200.26 (2.00)	198.60 (1.97)	202.90 (2.01)
	0.50	199.75 (1.99)	200.38 (1.99)	200.08 (1.98)	202.71 (2.02)
2	0.05	200.68 (2.01)	204.32 (2.04)	–	–
	0.10	200.95 (1.99)	200.69 (2.03)	204.49 (2.05)	–
	0.20	200.99 (1.98)	201.29 (2.00)	202.21 (2.03)	201.38 (2.01)
	0.50	199.63 (1.99)	199.53 (1.98)	200.46 (2.01)	202.46 (2.01)
3	0.05	200.52 (2.00)	197.40 (1.96)	–	–
	0.10	198.95 (1.96)	200.24 (1.99)	197.39 (1.96)	–
	0.20	198.89 (1.97)	197.94 (1.94)	201.70 (2.00)	–
	0.50	200.22 (1.99)	200.85 (1.98)	202.81 (2.01)	202.31 (2.01)
4	0.05	203.99 (2.06)	204.08 (2.04)	–	–
	0.10	203.23 (2.03)	204.58 (2.07)	204.11 (2.05)	–
	0.20	201.70 (2.00)	201.79 (2.03)	204.70 (2.07)	204.57 (2.05)
	0.50	200.38 (1.99)	200.25 (1.99)	201.40 (2.01)	201.52 (2.00)
5	0.05	200.19 (1.95)	201.23 (1.98)	–	–
	0.10	196.83 (1.89)	199.72 (1.94)	201.44 (1.98)	–
	0.20	198.23 (1.90)	194.82 (1.87)	200.59 (1.95)	199.59 (1.95)
	0.50	198.03 (1.91)	198.46 (1.92)	198.96 (1.93)	198.23 (1.93)
6	0.05	204.08 (2.03)	205.53 (2.04)	–	–
	0.10	205.43 (1.99)	205.78 (2.03)	205.81 (2.04)	–
	0.20	203.66 (1.99)	204.90 (1.97)	205.27 (2.02)	205.18 (2.04)
	0.50	202.98 (1.99)	202.03 (1.97)	201.49 (1.99)	204.47 (2.04)

Table A.3: Computing times (in seconds) of the charts EWMA-FD, EWMA-RS1, and EWMA-RS2 for computing their ARL_0 values. These values are the same as those in Figure 1 of the main article.

Cases	λ	EWMA-FD	EWMA-RS1	EWMA-RS2					
				$k = 0.005$	$k = 0.01$	$k = 0.05$	$k = 0.1$	$k = 0.2$	$k = 0.5$
2	0.01	218.71	4.03	0.16	0.06	–	–	–	–
	0.05	159.79	1.30	0.64	0.38	0.06	0.04	–	–
	0.10	148.89	0.69	0.57	0.45	0.15	0.06	0.04	–
	0.20	149.87	0.42	0.39	0.37	0.22	0.13	0.06	0.04
	0.30	152.39	0.31	0.32	0.31	0.23	0.16	0.09	0.04
	0.40	156.84	0.26	0.27	0.27	0.22	0.17	0.11	0.05
	0.50	163.68	0.24	0.24	0.24	0.20	0.17	0.12	0.06
3	0.01	210.51	2.46	0.12	0.06	–	–	–	–
	0.05	153.61	0.87	0.43	0.27	0.05	0.04	–	–
	0.10	143.81	0.51	0.40	0.32	0.11	0.05	0.04	–
	0.20	146.95	0.32	0.30	0.28	0.16	0.11	0.05	0.06
	0.30	146.46	0.26	0.25	0.25	0.19	0.13	0.08	0.04
	0.40	153.53	0.23	0.22	0.22	0.18	0.14	0.09	0.04
	0.50	157.97	0.21	0.21	0.20	0.17	0.15	0.11	0.05
4	0.01	275.51	4.24	0.16	0.06	–	–	–	–
	0.05	148.22	1.37	0.70	0.40	0.06	0.04	–	–
	0.10	138.45	0.63	0.49	0.39	0.12	0.06	0.04	–
	0.20	132.26	0.39	0.35	0.32	0.19	0.11	0.06	–
	0.30	136.44	0.29	0.28	0.27	0.20	0.15	0.08	0.04
	0.40	143.69	0.25	0.24	0.23	0.19	0.16	0.10	0.04
	0.50	146.13	0.22	0.22	0.21	0.18	0.16	0.11	0.05
5	0.01	215.14	3.55	0.14	0.06	–	–	–	–
	0.05	147.25	1.16	0.56	0.33	0.06	0.04	–	–
	0.10	138.45	0.63	0.49	0.39	0.12	0.06	0.04	–
	0.20	132.26	0.39	0.35	0.32	0.19	0.11	0.06	0.04
	0.30	136.44	0.29	0.28	0.27	0.20	0.15	0.08	0.04
	0.40	143.69	0.25	0.24	0.23	0.19	0.16	0.10	0.04
	0.50	146.13	0.22	0.22	0.21	0.18	0.16	0.11	0.05
6	0.01	220.62	5.37	0.22	0.08	–	–	–	–
	0.05	147.90	1.66	0.92	0.54	0.07	0.04	–	–
	0.10	138.60	0.92	0.77	0.61	0.18	0.07	0.04	–
	0.20	140.09	0.52	0.51	0.48	0.28	0.16	0.07	0.04
	0.30	147.79	0.39	0.40	0.38	0.29	0.20	0.11	0.04
	0.40	152.64	0.33	0.33	0.32	0.26	0.21	0.13	0.05
	0.50	158.66	0.28	0.29	0.29	0.24	0.21	0.15	0.06

Table A.4: Calculated optimal zero-state ARL_1 values and their standard errors (in the parentheses) of different control charts under different cases of serial data correlation. The nominal ARL_0 value of each chart is 200. The smallest optimal ARL_1 value among the seven charts is highlighted in bold in each case considered.

Cases	δ	EWMA-OR	EWMA-RSOR	EWMA-Z	EWMA-AR(1)	EWMA-FD	EWMA-RS1	EWMA-RS2
1	0.3	**24.91** (0.17)	35.98 (0.24)	**24.91** (0.17)	24.92 (0.17)	**24.91** (0.17)	35.98 (0.24)	35.92 (0.24)
	0.6	13.19 (0.07)	15.37 (0.09)	13.19 (0.07)	**12.27** (0.06)	13.19 (0.07)	15.37 (0.09)	15.10 (0.09)
	0.9	**7.85** (0.04)	8.81 (0.05)	**7.85** (0.04)	8.16 (0.04)	**7.85** (0.04)	8.81 (0.05)	8.55 (0.05)
	1.2	**5.36** (0.03)	5.89 (0.03)	**5.36** (0.03)	5.64 (0.03)	**5.36** (0.03)	5.89 (0.03)	5.61 (0.03)
	1.5	**3.94** (0.02)	4.26 (0.02)	**3.94** (0.02)	4.13 (0.02)	**3.94** (0.02)	4.26 (0.02)	4.04 (0.02)
2	0.3	41.97 (0.35)	59.99 (0.42)	41.97 (0.35)	**41.18** (0.35)	41.56 (0.35)	61.53 (0.46)	61.41 (0.46)
	0.6	20.84 (0.13)	28.93 (0.20)	20.84 (0.13)	**20.57** (0.13)	20.81 (0.13)	29.80 (0.20)	28.75 (0.21)
	0.9	13.59 (0.07)	17.04 (0.11)	13.59 (0.07)	**13.27** (0.07)	13.52 (0.07)	17.60 (0.12)	16.80 (0.12)
	1.2	10.11 (0.06)	11.14 (0.08)	10.11 (0.06)	**10.00** (0.06)	10.29 (0.06)	11.58 (0.08)	10.80 (0.08)
	1.5	7.29 (0.04)	7.79 (0.05)	7.29 (0.04)	**7.23** (0.04)	7.53 (0.05)	8.14 (0.05)	7.44 (0.05)
3	0.3	65.53 (0.65)	89.64 (0.73)	65.53 (0.65)	**64.96** (0.65)	66.44 (0.66)	89.59 (0.72)	89.84 (0.74)
	0.6	34.00 (0.28)	49.17 (0.37)	34.00 (0.28)	**33.78** (0.28)	34.79 (0.28)	50.13 (0.39)	49.68 (0.39)
	0.9	22.18 (0.15)	30.15 (0.24)	22.18 (0.15)	**21.68** (0.15)	22.94 (0.16)	31.24 (0.23)	30.70 (0.24)
	1.2	15.90 (0.09)	20.09 (0.18)	15.91 (0.09)	**15.42** (0.09)	16.61 (0.10)	21.44 (0.17)	20.51 (0.17)
	1.5	13.03 (0.10)	13.50 (0.12)	13.03 (0.10)	**12.71** (0.09)	12.82 (0.07)	15.36 (0.12)	14.45 (0.16)
4	0.3	39.57 (0.32)	57.49 (0.41)	39.57 (0.32)	**39.41** (0.33)	39.57 (0.33)	58.89 (0.43)	58.82 (0.43)
	0.6	19.75 (0.12)	27.54 (0.18)	19.75 (0.12)	**19.55** (0.12)	19.80 (0.12)	28.17 (0.19)	27.27 (0.19)
	0.9	12.97 (0.07)	16.22 (0.11)	12.96 (0.07)	**12.68** (0.07)	12.90 (0.07)	16.64 (0.11)	15.88 (0.11)
	1.2	9.62 (0.06)	10.68 (0.07)	9.62 (0.06)	**9.51** (0.06)	9.71 (0.06)	11.03 (0.07)	10.33 (0.07)
	1.5	7.05 (0.04)	7.59 (0.05)	7.05 (0.04)	**6.96** (0.04)	7.19 (0.04)	7.85 (0.05)	7.24 (0.05)
5	0.3	47.86 (0.42)	68.95 (0.52)	47.86 (0.42)	**47.25** (0.41)	47.89 (0.42)	69.93 (0.53)	69.96 (0.53)
	0.6	23.91 (0.16)	34.44 (0.22)	23.91 (0.16)	**23.58** (0.16)	23.96 (0.16)	35.39 (0.23)	35.01 (0.25)
	0.9	15.37 (0.08)	20.80 (0.13)	15.37 (0.08)	**15.06** (0.08)	15.45 (0.09)	21.48 (0.15)	20.77 (0.14)
	1.2	12.21 (0.07)	13.63 (0.09)	12.21 (0.07)	11.96 (0.07)	**11.27** (0.05)	14.25 (0.09)	13.45 (0.09)
	1.5	8.76 (0.05)	9.45 (0.06)	8.76 (0.05)	**8.61** (0.05)	9.17 (0.05)	10.13 (0.07)	9.13 (0.06)
6	0.3	26.34 (0.19)	38.95 (0.26)	27.34 (0.19)	27.00 (0.19)	**26.34** (0.19)	39.22 (0.28)	39.20 (0.28)
	0.6	12.99 (0.07)	16.68 (0.10)	13.42 (0.07)	13.28 (0.07)	**12.98** (0.07)	16.83 (0.10)	16.34 (0.11)
	0.9	**8.51** (0.05)	9.58 (0.06)	8.64 (0.05)	8.90 (0.05)	**8.51** (0.05)	9.60 (0.06)	9.23 (0.06)
	1.2	**5.76** (0.03)	6.30 (0.04)	**5.76** (0.03)	6.01 (0.03)	**5.76** (0.03)	6.34 (0.04)	6.01 (0.04)
	1.5	4.18 (0.02)	4.51 (0.03)	**4.17** (0.02)	4.35 (0.02)	**4.17** (0.02)	4.52 (0.03)	4.26 (0.03)

Table A.5: Calculated actual ATS_0 values and their standard errors (in the parentheses) of the charts CUSUM-RS, EWMA-RS1 and EWMA-RS2 in Setting (i) of the observation times. The nominal ATS_0 value of each chart is fixed at 200.

Cases	k	CUSUM-RS	λ	EWMA-RS1	EWMA-RS2					
					$k = 0.005$	$k = 0.01$	$k = 0.05$	$k = 0.1$	$k = 0.2$	$k = 0.5$
1	0.25	200.25 (1.91)	0.05	200.69 (1.88)	201.02 (1.93)	199.83 (1.95)	199.14 (1.98)	204.57 (2.03)	–	–
	0.50	198.41 (1.95)	0.10	197.51 (1.91)	199.27 (1.94)	198.40 (1.93)	200.90 (1.99)	199.83 (1.98)	204.51 (2.03)	–
	0.75	200.17 (1.98)	0.20	201.91 (2.00)	201.53 (2.00)	200.66 (1.99)	199.75 (1.98)	200.26 (2.00)	198.60 (1.97)	202.90 (2.01)
	1.00	199.61 (1.99)	0.50	197.94 (1.97)	198.42 (1.97)	198.07 (1.96)	199.75 (1.99)	200.38 (1.99)	200.08 (1.98)	202.71 (2.02)
2	0.25	198.99 (1.91)	0.05	201.70 (1.90)	199.56 (1.91)	199.20 (1.97)	200.68 (2.01)	204.32 (2.04)	–	–
	0.50	198.23 (1.95)	0.10	199.21 (1.93)	198.31 (1.94)	197.15 (1.92)	200.95 (1.99)	200.69 (2.03)	204.49 (2.05)	–
	0.75	201.63 (1.99)	0.20	198.56 (1.95)	197.76 (1.95)	197.28 (1.95)	200.99 (1.98)	201.29 (2.00)	202.21 (2.03)	201.38 (2.01)
	1.00	199.34 (1.97)	0.50	201.61 (2.01)	201.98 (2.02)	201.44 (2.01)	199.63 (1.99)	199.53 (1.98)	200.46 (2.01)	202.46 (2.01)
3	0.25	198.15 (1.91)	0.05	202.91 (1.93)	200.28 (1.93)	199.86 (1.96)	200.52 (2.00)	197.40 (1.96)	–	–
	0.50	198.50 (1.98)	0.10	199.32 (1.93)	200.50 (1.95)	198.52 (1.95)	198.95 (1.96)	200.24 (1.99)	197.39 (1.96)	–
	0.75	199.66 (1.98)	0.20	197.74 (1.96)	196.91 (1.97)	196.13 (1.96)	198.89 (1.97)	197.94 (1.94)	201.70 (2.00)	–
	1.00	198.46 (1.97)	0.50	201.38 (2.01)	201.61 (2.01)	202.26 (2.02)	200.22 (1.99)	200.85 (1.98)	202.81 (2.01)	202.31 (2.01)

Table A.6: Calculated actual ATS_0 values and their standard errors (in the parentheses) of the charts CUSUM-RS, EWMA-RS1 and EWMA-RS2 in Setting (ii) of the observation times. The nominal ATS_0 value of each chart is fixed at 200.

Cases	k	CUSUM-RS	λ	EWMA-RS1	EWMA-RS2					
					$k = 0.005$	$k = 0.01$	$k = 0.05$	$k = 0.1$	$k = 0.2$	$k = 0.5$
1	0.25	207.44 (3.17)	0.05	201.25 (1.56)	200.26 (1.53)	199.80 (1.51)	200.10 (1.43)	201.27 (1.41)	202.01 (1.41)	–
	0.50	207.26 (3.22)	0.10	201.36 (1.48)	201.35 (1.47)	200.88 (1.46)	201.05 (1.39)	200.87 (1.36)	201.71 (1.32)	203.85 (1.32)
	0.75	205.20 (3.21)	0.20	200.88 (1.62)	200.87 (1.61)	200.99 (1.61)	202.08 (1.59)	202.91 (1.57)	201.80 (1.52)	203.42 (1.47)
	1.00	204.01 (3.18)	0.50	206.80 (2.50)	206.71 (2.50)	206.72 (2.50)	206.08 (2.49)	205.52 (2.47)	206.64 (2.46)	204.24 (2.39)
2	0.25	204.83 (2.94)	0.05	203.29 (1.47)	203.79 (1.46)	203.12 (1.44)	201.73 (1.33)	203.10 (1.29)	202.26 (1.26)	–
	0.50	203.25 (2.91)	0.10	203.30 (1.41)	203.13 (1.41)	203.11 (1.39)	203.59 (1.35)	202.67 (1.30)	202.46 (1.24)	204.26 (1.23)
	0.75	204.96 (2.97)	0.20	204.90 (1.57)	205.13 (1.57)	204.81 (1.56)	204.96 (1.53)	205.39 (1.51)	204.60 (1.46)	205.12 (1.40)
	1.00	200.96 (2.93)	0.50	203.20 (2.36)	203.35 (2.36)	203.43 (2.36)	203.91 (2.36)	204.08 (2.35)	203.15 (2.32)	204.39 (2.29)
3	0.25	205.64 (2.76)	0.05	200.34 (1.41)	199.94 (1.39)	200.26 (1.36)	201.13 (1.23)	199.71 (1.14)	201.55 (1.08)	–
	0.50	202.25 (2.64)	0.10	199.25 (1.32)	199.54 (1.31)	199.73 (1.30)	199.91 (1.23)	200.88 (1.18)	201.99 (1.10)	202.07 (1.06)
	0.75	205.74 (2.65)	0.20	202.27 (1.47)	202.48 (1.46)	202.34 (1.45)	202.49 (1.41)	202.13 (1.36)	201.57 (1.30)	203.39 (1.26)
	1.00	206.44 (2.69)	0.50	204.88 (2.19)	205.12 (2.19)	205.01 (2.19)	205.79 (2.18)	206.20 (2.17)	206.47 (2.12)	207.13 (2.08)

Table A.7: Computing times (in seconds) of the charts CUSUM-RS, EWMA-RS1, and EWMA-RS2 for computing their ATS_0 values in Setting (i) of the observation times.

Cases	k	CUSUM-RS	λ	EWMA-RS1	EWMA-RS2					
					$k = 0.005$	$k = 0.01$	$k = 0.05$	$k = 0.1$	$k = 0.2$	$k = 0.5$
1	0.25	0.56	0.05	1.66	0.87	0.52	0.07	0.04	–	–
	0.50	0.22	0.10	0.88	0.73	0.58	0.19	0.07	0.04	0.42
	0.75	0.12	0.20	0.53	0.50	0.47	0.28	0.17	0.07	0.04
	1.00	0.07	0.50	0.28	0.28	0.28	0.24	0.21	0.15	0.06
2	0.25	0.39	0.05	1.30	0.64	0.38	0.06	0.04	–	–
	0.50	0.16	0.10	0.69	0.57	0.45	0.15	0.06	0.04	–
	0.75	0.09	0.20	0.42	0.39	0.37	0.22	0.13	0.06	0.04
	1.00	0.06	0.50	0.24	0.24	0.24	0.20	0.17	0.12	0.06
3	0.25	0.25	0.05	0.87	0.43	0.27	0.05	0.04	–	–
	0.50	0.12	0.10	0.51	0.40	0.32	0.11	0.05	0.04	–
	0.75	0.07	0.20	0.32	0.30	0.28	0.16	0.11	0.05	0.06
	1.00	0.05	0.50	0.21	0.21	0.20	0.17	0.15	0.11	0.05

Table A.8: Computing times (in seconds) of the charts CUSUM-RS, EWMA-RS1, and EWMA-RS2 for computing their ATS_0 values in Setting (ii) of the observation times.

Cases	k	CUSUM-RS	λ	EWMA-RS1	EWMA-RS2					
					$k = 0.005$	$k = 0.01$	$k = 0.05$	$k = 0.1$	$k = 0.2$	$k = 0.5$
1	0.25	0.08	0.05	0.16	0.15	0.13	0.07	0.04	0.02	–
	0.50	0.04	0.10	0.12	0.12	0.11	0.08	0.06	0.04	0.02
	0.75	0.02	0.20	0.09	0.09	0.09	0.08	0.06	0.05	0.03
	1.00	0.01	0.50	0.06	0.06	0.06	0.05	0.05	0.04	0.03
2	0.25	0.08	0.05	0.15	0.14	0.12	0.07	0.04	0.02	–
	0.50	0.04	0.10	0.11	0.11	0.10	0.07	0.06	0.04	0.02
	0.75	0.02	0.20	0.09	0.08	0.08	0.07	0.06	0.04	0.03
	1.00	0.01	0.50	0.06	0.06	0.05	0.05	0.05	0.04	0.03
3	0.25	0.06	0.05	0.12	0.11	0.10	0.06	0.04	0.02	–
	0.50	0.03	0.10	0.10	0.09	0.09	0.06	0.05	0.03	0.02
	0.75	0.02	0.20	0.08	0.08	0.07	0.06	0.05	0.04	0.03
	1.00	0.01	0.50	0.05	0.05	0.05	0.05	0.05	0.04	0.02

Figure A.1: Optimal values of λ used in EWMA-RS1 and optimal values of λ and k used in EWMA-RS2 in various cases considered in Figure A.1.

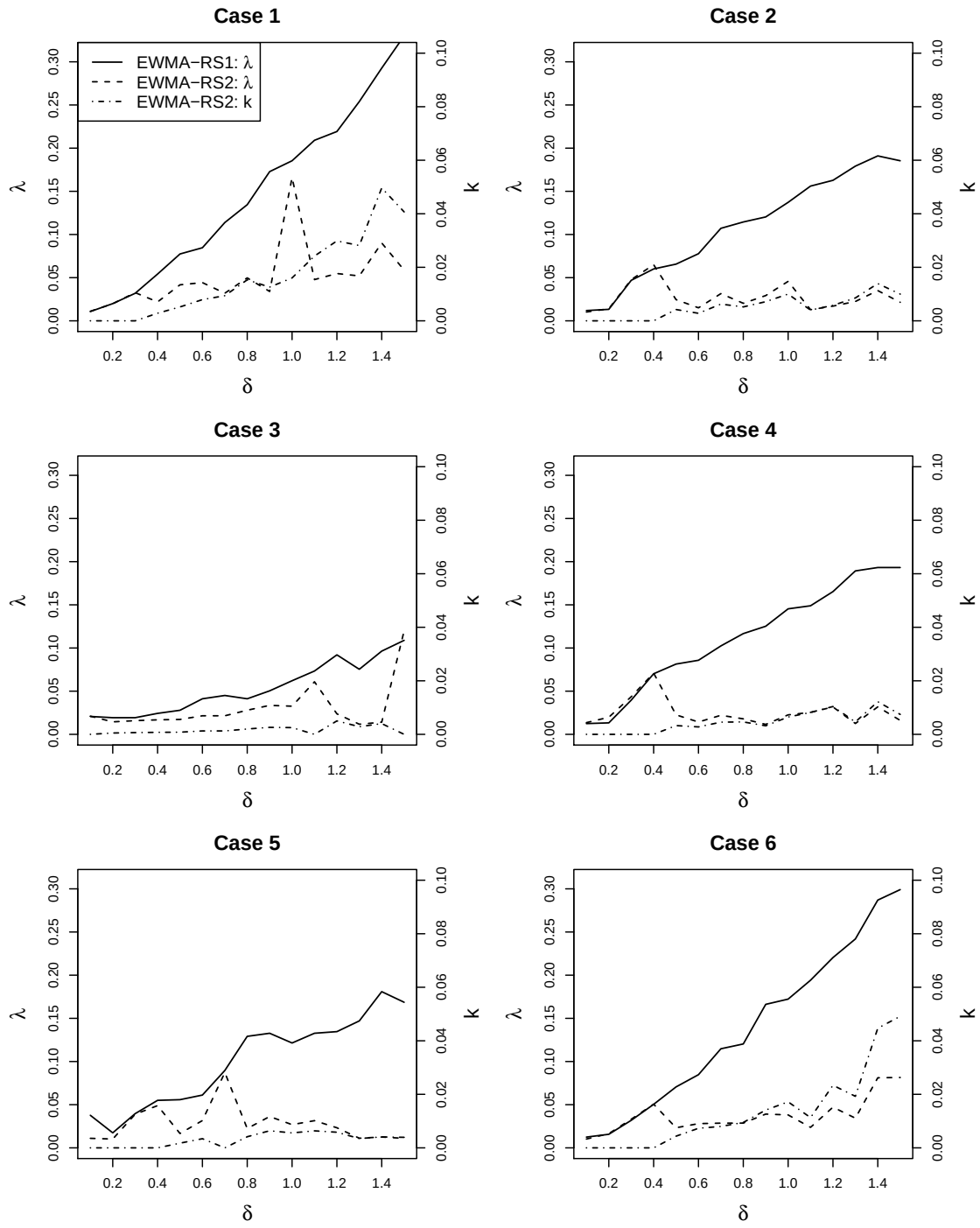

Data Availability Statement

The Sea Surface Temperature datasets analyzed during this study are available in R package **tseries** on the CRAN. Sample codes related to the proposed method and the results shown in the simulation study can be found in the online supplementary file.

Conflict of Interest

The authors have no conflict of interest.

Acknowledgments

We thank the editor and reviewers for their potential comments and suggestions. No funding was received.

References

Apley, D. W. and Tsung, F. (2002), "The autoregressive T^2 chart for monitoring univariate autocorrelated processes," *Journal of Quality Technology*, **34**, 80–96.

Cane, M. A. (2005), "The evolution of El Niño, past and future," *Earth and Planetary Science Letters*, **230**, 227–240.

Capizzi, G. and Masarotto, G. (2008), "Practical design of generalized likelihood ratio control charts for autocorrelated data," *Technometrics*, **50**, 357–370.

Capizzi, G. and Masarotto, G. (2016), "Efficient control chart calibration by simulated stochastic approximation," *IIE Transactions*, **48**, 57–65.

Caviedes, C. N. (1984), "El Nino 1982-83," *Geographical Review*, **74**, 267–290.

Chatterjee, S. and Qiu, P. (2009), "Distribution-free cumulative sum control charts using bootstrap-based control limits," *Annals of Applied Statistics*, **3**, 349–369.

Chou, Y. M., Polansky, A. M., and Mason, R. L. (1998), "Distribution-free cumulative sum control charts using bootstrap-based control limits," *Journal of Quality Technology*, **30**, 133–141.

Crowder, S. V. (1989), "Design of exponentially weighted moving average schemes," *Journal of Quality Technology*, **21**, 155–162.

Crowder, S. V. and Hamilton, M. D. (1992), "An EWMA for monitoring a process standard deviation," *Journal of Quality Technology*, **24**, 12–21.

Gan, F. (1998), "Designs of one-and two-sided exponential EWMA charts," *Journal of Quality Technology*, **30**, 55–69.

Glantz, M. H. (2001), *Currents of Change: Impacts of El Niño and La Niña on Climate and Society*, Cambridge: Cambridge University Press.

Hawkins, D. M. and Olwell, D. H. (1998), *Cumulative Sum Charts and Charting for Quality Improvement*, New York: sprinter.

Johnson, N. L. (1949), "Systems of frequency curves generated by methods of translation," *Biometrika*, **36**, 149–176.

Kim, S. H., Alexopoulos, C., Tsui, K. L., and Wilson, J. R. (2007), "A distribution-free tabular CUSUM chart for autocorrelated data," *IIE Transactions*, **39**, 317–330.

Lahiri, S. N. (2003), *Resampling Methods for Dependent Data*, New York: sprinter.

Lee, H. C. and Apley, D. W. (2011), "Improved design of robust exponentially weighted moving average control charts for autocorrelated processes," *Quality and Reliability Engineering International*, **27**, 337–352.

Li, J. and Qiu, P. (2016), "Nonparametric dynamic screening system for monitoring correlated longitudinal data," *IIE Transactions*, **48**, 772–786.

Li, W. and Qiu, P. (2020), "A general charting scheme for monitoring serially correlated data with short-memory dependence and nonparametric distributions," *IISE Transactions*, **52**, 61–74.

Luersen, M. A., Le Riche, R., and Guyon, F. (2004), "A constrained, globalized, and bounded Nelder–Mead method for engineering optimization," *Structural and Multidisciplinary Optimization*, **27**, 43–54.

Montgomery, D. C. (2019), *Introduction to Statistical Quality Control*, New York: John Wiley & Sons.

Qiu, P. (2008), "Distribution-free multivariate process control based on log-linear modeling," *IIE Transactions*, **40**, 664–677.

Qiu, P. (2014), *Introduction to Statistical Process Control*, Boca Raton, FL: Chapman Hall/CRC.

Qiu, P., Zi, X., and Zou, C. (2018), "Nonparametric dynamic curve monitoring," *Technometrics*, **60**, 386–397.

Qiu, P., Li, W., and Li, J. (2020), "A new process control chart for monitoring short-range serially correlated data," *Technometrics*, **62**, 71–83.

Qiu, P. and Xie, X. (2022), "Transparent sequential learning for statistical process control of serially correlated data," *Technometrics*, **64**, 487–501.

Runger, G. C. and Willemain, T. R. (1995), "Model-based and model-free control of autocorrelated processes," *Journal of Quality Technology*, **27**, 283–292.

Trenberth, K. E. and Hoar, T. J. (1997), "El Niño and climate change," *Geophysical Research Letters*, **24**, 3057–3060.

Xie, X. and Qiu, P. (2022), "Robust monitoring of multivariate processes with short-ranged serial data correlation," *Quality and Reliability Engineering International*, **38**, 4196–4209.

Xue, L. and Qiu, P. (2021), "A nonparametric CUSUM chart for monitoring multivariate serially correlated processes," *Journal of Quality Technology*, **53**, 396–409.

You, L. and Qiu, P. (2019), "Fast computing for dynamic screening systems when analyzing correlated data," *Journal of Statistical Computation and Simulation*, **89**, 379–394.

You, L. and Qiu, P. (2020), "An effective method for online disease risk monitoring," *Technometrics*, **62**, 249–264.

Zhang, N. F. (1998), "A statistical control chart for stationary process data," *Technometrics*, **40**, 24–38.